Int J Adv Manuf Technol (2016) 85:2805–2818
DOI 10.1007/s00170-015-8133-8

ORIGINAL ARTICLE

Energy modeling for variable material removal rate machining process: an end face turning case

Shun Jia [1,2] · **Renzhong Tang** [1] · **Jingxiang Lv** [3] · **Zhongwei Zhang** [1] · **Qinghe Yuan** [2]

Received: 19 July 2015 / Accepted: 12 November 2015 / Published online: 25 November 2015

Abstract Material-cutting energy modeling is the key technology of energy modeling of machining process, being the foundation of energy optimization. The material-cutting power changes dynamically during variable-material removal rate (MRR) machining process. Hence, the energy characteristic of variable-MRR machining process is more complicated than that of constant-MRR machining process. In this paper, a modeling method of material-cutting energy for variable-MRR machining process is proposed. The dynamic power characteristics are fully considered in this method, and the impacts of cutting parameters on material-cutting energy are also considered. Experimental studies were conducted to obtain the fitting coefficients of the proposed energy model. Finally, energy calculations of four actual end face turning processes were performed. The results show that the predictive accuracy of all tested end face turning cases is above 90 %. The proposed method provides an accurate energy model for process planning in metal cutting process, which helps manufacturers determinate the energy-optimal process plan.

✉ Renzhong Tang
tangrz@zju.edu.cn

Shun Jia
herojiashun@163.com

[1] Industrial Engineering Center, Zhejiang Province Key Laboratory of Advanced Manufacturing Technology, Zhejiang University, Hangzhou 310027, China

[2] Shandong University of Science and Technology, Qingdao 266590, China

[3] Xi'an Research Institute of Navigation Technology, Xi'an 710068, China

Keywords Machining · Material removal rate (MRR) · Cutting energy · Sustainable production · Low carbon manufacturing

Nomenclature

a_p	Depth of cut (mm)
$a_p(t)$	Functions of depth of cut against time
$\overline{a_{pi}}$	Average depth of cut of subinterval i (mm)
C_{Fc}	Constant
d_0	Diameter of workpiece (mm)
E_{MC}	Material-cutting energy (J)
f	Feed rate (mm/r)
$f(t)$	Functions of feed rate against time
$\overline{f_i}$	Average feed rate of subinterval i (mm/r)
F_c	Main cutting force (N)
k_{Fc}	Correction coefficient
l	Feed distance during cutter entering stage (mm)
MRR	Material removal rate (cm^3/s)
$\overline{MRR}$	Average material removal rate (cm^3/s)
n	Spindle speed (r/min)
n_{Fc}	Constant
N	Number of subintervals
P_{MC}	Material-cutting power (W)
P_{MC_d}	Material-cutting power in dry environment (W)
P_{MC_w}	Material-cutting power in wet environment (W)
$\overline{P_{MC}}$	Average material-cutting power (W)
$\overline{P_{MC\_d}}$	Average material-cutting power in dry environment (W)
$\overline{P_{MC\_w}}$	Average material-cutting power in wet environment (W)
P_{Tcut}	Theoretical cutting power (W)
SCE	Specific cutting energy (kJ/cm^3)
t	Cutting time (s)
t_{en}	Duration of cutter entering stage (s)

t_{fcut}	Duration of fully cutting stage (s)
T	Duration of variable-MRR machining process (s)
v_0	Initial cutting speed (m/min)
v_c	Cutting speed (m/min)
$v_c(t)$	Functions of cutting speed against time
$\overline{v_{ci}}$	Average cutting speed of subinterval i (m/min)
v_f	Feed speed (mm/s)
x_{Fc}	Constant
y_{Fc}	Constant
α	Constant
α_0	Coefficient of power loss
β	Constant
γ	Constant
λ	Constant
λ_0	Constant (J/cm^3)
k_r	Main angle (°)
Δt	Duration of each subinterval (s)

1 Introduction

Manufacturing consumes significant amounts of energy and releases large amounts of wastes (e.g., solid, liquid, and gaseous wastes), resulting in substantial stress on the environment [1]. Machining represents one of the main energy-consuming activities in manufacturing industries, and energy consumption determines 20 % of machine tool operating cost [2]. It is noted that computer numerical control (CNC) machining is one of the fundamental machining technologies, and its impacts to the environment are mainly attributed to electrical energy use [3]. Much of our electricity is still produced from carbon intensive sources in the foreseeable future, and CO_2 is emitted into the atmosphere adding to the effect of global warming during the production process of electricity [4, 5]. According to the report of the International Energy Agency (IEA), the manufacturing industry is responsible for nearly one third of global energy consumption and 36 % of global CO_2 emission [6]. It is clear to see that the manufacturing industry has become one of the major sources of energy consumption and carbon emissions. Hence, sustainable manufacturing technique has drawn more and more attention in manufacturing industries. Reducing the energy consumed by machining processes has been identified as one of the strategies to significantly improve the environmental performance of manufacturing processes and systems [7, 8].

The first step towards reducing and optimizing the energy consumption in machining is to analyze the impact of machining parameters on energy consumption [9]. Hence, power and energy modeling method of machining process is the foundation of the energy reduction and optimization of manufacturing processes. An accurate energy consumption model could improve energy forecasting of machining processes or in early product design stage, consequently, makes it possible to select the most energy efficient option [10]. According to the characteristic of material removal rate (MRR), machining processes can be grouped into two types: constant-MRR machining process and variable-MRR machining process. Constant-MRR machining process is defined as the process that all of the cutting parameters remain unchanged during machining. Variable-MRR machining process is defined as the process that at least one of the cutting parameters changes with time during machining. As shown in Fig. 1, taking turning process as an example where the cutting parameters are cutting speed v_c, feed rate f and depth of cut a_p, the power characteristics of these two types of processes are different. The power of constant-MRR process is a stable value, while the power of variable-MRR process changes over time and the power characteristic is more complicated. Moreover, the total cutting power of machining process can be divided into two parts: air-cutting power and material-cutting power [11–13]. Air-cutting power is the power demand while following the same tool path and using the same cutting parameters without material removal. The difference between total cutting power and air-cutting power is the power required for material removal (material-cutting power) [14]. The material-cutting power is the main factor resulting in the difference between the cutting power of variable-MRR machining process and constant-MRR machining process. Therefore, material-cutting energy is focused in this study. The aim is to propose a modeling method of material-cutting energy for variable-MRR machining processes.

The remainder of this paper is organized as follows. Literature review is presented in the next section. Then, detailed discussions of the material-cutting energy model for variable-MRR machining processes are given in Section 3, followed by the experimental study to obtain the fitting coefficients of the developed material-cutting energy model in Section 4. Finally, the conclusions and future research directions are summarized in Section 5.

2 Literature review

Power or energy modeling and energy efficiency issues of machining processes have been discussed in some existing literatures [15–19]. Extensive experiments were conducted by Gutowski et al. [20, 21], and a linear function between cutting power and MRR was developed. It was shown that the cutting power is mainly affected by MRR. Kara and Li [14, 22] investigated the relationship between specific energy consumption (SEC) and MRR. Curve estimation indicated that inverse model ($SEC = C_0 + C_1/MRR$) provides the best fitness between SEC and MRR [14]. An improved energy consumption model was proposed by Balogun et al. [23] based on the model developed by Gutowski. Basic power, ready state power, and coolant pumping power were also

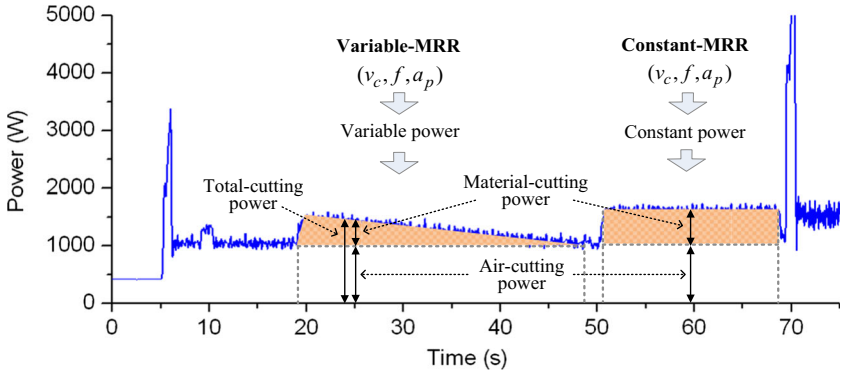

Fig. 1 Power profiles of variable-MRR process vs. constant-MRR process

included in their improved model. Similarly, another improved power model was proposed to estimate the energy consumption of a CNC milling machine as function of MRR and spindle speed n ($P = P_{standby} + k_1 n + b + k_0 MRR$) [10]. However, the improved models provided by Balogun et al. [23] and Li et al. [10] were both based on the MRR, which was viewed as a single variable. Actually, MRR is determined by the co-effect of cutting speed v_c, feed rate f, and depth of cut a_p. The effect of each cutting parameter (v_c, f, a_p) was not fully considered in the previous two improved models. In the work of Jia [13], the effect of cutting speed, feed rate, and depth of cut were all taken into account to establish the material-cutting power model. An exponential model was developed between material-cutting power and three cutting parameters (v_c, f, a_p). However, it is only used to calculate the power of the constant-MRR machining process (e.g., external turning process).

As mentioned previously, the energy consumption characteristics of constant-MRR machining process and variable-MRR machining process are different. Most of existing studies focused on power or energy modeling of constant-MRR machining processes, e.g., external turning [14, 24], face milling [25–29], etc. The cutting speed v_c, feed rate f, and depth of cut a_p in constant-MRR machining process are all constant. Hence, the cutting power is a constant value during cutting process. The situation is significantly different, when it comes to variable-MRR process. As the MRR is changing during machining process (at least one of three cutting parameters is changing during machining), cutting force will change with the varying cutting parameters. Consequently, the cutting power will be a dynamic changing value as well. For instance, end face turning, grooving, and chamfering are typical variable-MRR machining processes. It is easy to be seen that energy models of variable-MRR machining process are more complicated than that of constant-MRR machining process. The energy modeling methods used for constant-MRR machining process can provide certain reference value for variable-MRR machining process. Up to now, research specially focused on the energy modeling method of variable-MRR machining processes is really rare. The power profiles of end face turning were mentioned in Liu et al. [30]; however, detailed information of power model for end face turning was not provided. Hu et al. [31] proposed an online energy efficiency monitoring approach of machine tools, where the total energy consumption of machine tool is obtained based on the constant energy (measured in advance) as well as the variable energy (estimated online according to power balance equation and additional load loss function). Tristo et al. [32] established an online power consumption monitoring system to analyze the energy efficiency in microelectrical discharge machining process. The realization of the above two approaches are dependent on the online power monitoring of machine tool. Machining parameters optimization considering energy consumption for machining processes was conducted by several researchers [9, 33–35]. However, the energy model of variable-MRR machining process was not mentioned in the above energy optimization related references. A Therblig-based energy modeling method of machining process was proposed by Jia et al. [36]. In the above paper, power calculations of several variable-MRR processes (end face turning and grooving process) were mentioned, and simplified models were used for computing the power of variable-MRR processes (average material-cutting power was obtained by using average-MRR as a variable). Diaz et al. [37] divided variable-MRR milling process into multiple subintervals and established the relationship between average energy consumption and average-MRR in each subinterval. However, the MRR was considered as a single parameter in both aforementioned two methods. As mentioned previously, the MRR is simultaneously influenced by cutting speed v_c, feed rate f, and depth of cut a_p. More important, the impact characteristics of these cutting parameters on the material-cutting power are not the same. Hence, an improved material-cutting energy modeling method for variable-MRR machining process is proposed based on the decomposed MRR in this study. The variable-MRR machining processes are decomposed into N subintervals, and the function between material-cutting power and cutting parameters (v_c, f, a_p) is established in each subinterval by fully considering the impacts of three cutting parameters on the material-cutting power. Consequently, the material-cutting

energy model of the variable-MRR machining process can further be built.

3 Modeling methodology

3.1 Material-cutting energy model for general variable-MRR process

The material-cutting power of the variable-MRR process changes with time during machining due to the dynamic changing cutting parameters. The power profile of a common variable-MRR machining process is shown in Fig. 2. The material-cutting power is the main factor resulting in the difference between the cutting power of variable-MRR machining processes and constant-MRR machining processes. Understanding the characteristic of material-cutting power is helpful to the material-cutting energy modeling. This section focuses on the material-cutting energy modeling method for variable-MRR processes.

3.1.1 Average-MRR based model

Material-cutting power changes with time during the variable-MRR machining process due to the changing MRR (as shown in Fig. 3). Based on the references [36, 38–40], the relationship model between material-cutting power and MRR can be established.

$$P_{MC} = 1000 \cdot (1 + \alpha_0) \cdot \mathrm{SCE} \cdot \mathrm{MRR} \tag{1}$$

Where P_{MC} is material-cutting power, W; α_0 is coefficient of power loss; *SCE* is specific cutting energy, kJ/cm^3; *MRR* is material removal rate, cm^3/s.

To simplify the analysis of the material-cutting power of variable-MRR machining process, average-MRR of the cutting process is viewed as a single parameter. Based on formula (1), the function between average material-cutting power and average-MRR can be expressed as follows:

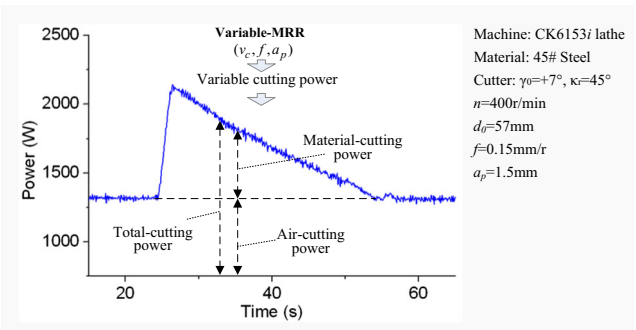

Fig. 2 Power profile of a common variable-MRR machining process

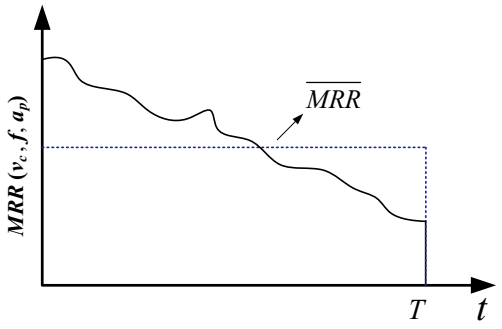

Fig. 3 Schematic diagram of average-MRR

$$\overline{P_{MC}} = \lambda_0 \cdot \overline{\mathrm{MRR}} \tag{2}$$

Where $\overline{P_{MC}}$ is average material-cutting power, W; λ_0 is a constant, J/cm^3; $\overline{\mathrm{MRR}}$ is average material removal rate, cm^3/s. The equation $\lambda_0 = 1000 \cdot (1 + \alpha_0) \cdot SCE$ is satisfied.

Energy consumption of the variable-MRR machining process can be calculated as follows:

$$E_{MC} = \lambda_0 \cdot \overline{\mathrm{MRR}} \cdot T \tag{3}$$

Where E_{MC} is material-cutting energy of variable-MRR machining process, J; T is duration of variable-MRR machining process, *s*.

Based on Eqs. (2) and (3), the material-cutting energy of variable-MRR machining process can be obtained. However, the disadvantages of the above simplified average model are as follows: (1) MRR is essentially determined by the co-effect of cutting parameters, but MRR was simplified as a single variable in the above model. Consequently, the effect of each cutting parameter (v_c, f, a_p) on material-cutting power was not fully considered. (2) As the obtained power is the average material-cutting power, the dynamic changing of material-cutting power of machining process cannot be reflected, and it is hard to know the energy distribution of the whole machining process. In order to deal with the above problems, an improved material-cutting energy model is proposed in next subsection.

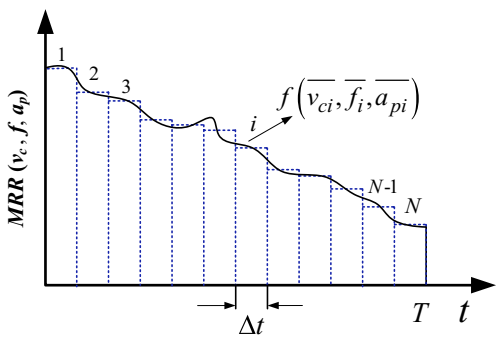

Fig. 4 Schematic diagram of decomposed-MRR

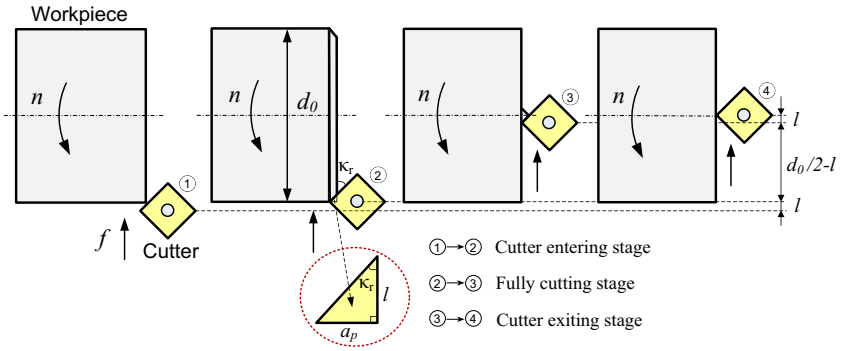

Fig. 5 Three stages of a typical end face turning process

3.1.2 Improved energy model

As shown in Fig. 4, the variable-MRR machining process is decomposed into N subintervals to investigate its energy consumption. The variations of cutting parameters (v_c, f, a_p) in each subinterval will be very small if the value of N is large enough. The actual value of each cutting parameter can be substituted by the average value of corresponding parameter in each subinterval. Hence, it can be treated as a constant-MRR machining process within each subinterval. The larger the N is, the more each subinterval is close to a constant-MRR machining process.

According to the references [39, 41], material-cutting power can be expressed as follows:

$$P_{MC} = (1 + \alpha_0) P_{Tcut} \tag{4}$$

Where PT_{cut} is theoretical cutting power and also the minimum power required for material removing, W. α_0 is the coefficient of power loss.

The theoretical cutting power is generated by cutting force, which includes main cutting force, radial cutting force, and axial cutting force. Main cutting force is responsible for 9 ~ 99 % of the generation of total power [42]. Therefore, the theoretical cutting power can be written as follows:

$$P_{Tcut} = F_c \cdot v_c / 60 \tag{5}$$

Where F_c is main cutting force, N; v_c is cutting speed, m/min.

The main cutting force can further be represented as Eq. 6 [43], which is a commonly used empirical formula taking the influence of the three cutting parameters (v_c, f and a_p) into account.

$$F_c = k_{Fc} \cdot C_{Fc} \cdot v_c^{n_{Fc}} \cdot f^{y_{Fc}} \cdot a_p^{x_{Fc}} \tag{6}$$

Where F_c is main cutting force, N; k_{Fc} is correction coefficient; C_{Fc}, n_{Fc}, y_{Fc}, x_{Fc} are constants; v_c is cutting speed, m/min; f is feed rate, mm/r; α_p is depth of cut, mm.

Based on Eqs. (4) ~ (6), the material-cutting power can further be written as follows:

$$\begin{aligned} P_{MC} &= (1 + \alpha_0) \cdot F_c \cdot v_c / 60 \\ &= (1 + \alpha_0) \cdot k_{Fc} \cdot C_{Fc} \cdot v_c^{n_{Fc}+1} \cdot f^{y_{Fc}} \cdot a_p^{x_{Fc}} / 60 \end{aligned} \tag{7}$$

The material-cutting power can also be expressed as follows:

$$P_{MC} = \lambda \cdot v_c^{\alpha} \cdot f^{\beta} \cdot a_p^{\gamma} \tag{8}$$

Where λ, α, β and γ are constants; the following equations are satisfied: $\lambda = (1 + \alpha_0) \cdot k_{Fc} \cdot C_{Fc}/60$, $\alpha = n_{Fc} + 1$, $\beta = y_{Fc}$, $\gamma = x_{Fc}$.

As each subinterval of variable-MRR machining process is treated as a constant-MRR machining process, average material-cutting power of subinterval i can be expressed as Eq. (9) based on formula (8):

$$\overline{P_{MC,\,i}} = \lambda \cdot \overline{v_{ci}}^{\,\alpha} \cdot \overline{f_i}^{\,\beta} \cdot \overline{a_{pi}}^{\,\gamma} \tag{9}$$

Where $\overline{v_{ci}}$ is average cutting speed of subinterval i, m/min; $\overline{f_i}$ is average feed rate of subinterval i, mm/r; $\overline{a_{pi}}$ is average depth of cut of subinterval i, mm.

Table 1 Material-cutting energy model for end face turning process

Item	Material-cutting energy model
Average-MRR based model	$E_{MC} = \lambda_0 \cdot \overline{MRR} \cdot T, \quad \left(\overline{MRR} = \frac{\pi d_0^2 \times a_p}{4000 \times T}, \quad T = t_{en} + t_{fcut}\right)$
Improved energy model	$E_{MC} = \int_0^{t_{en}} \left[\lambda \cdot \left(v_0 - \frac{2f\pi n^2}{60000} t\right)^{\alpha} \cdot f^{\beta} \cdot (a_p \cdot t / t_{en})^{\gamma}\right] dt + \int_{t_{en}}^{t_{en}+t_{fcut}} \left[\lambda \cdot \left(v_0 - \frac{2f\pi n^2}{60000} t\right)^{\alpha} \cdot f^{\beta} \cdot a_p^{\gamma}\right] dt$

Table 2 Process parameters and their levels

Factors	Parameters	Level 1	Level 2	Level 3
A	n (r/min)	400	600	800
B	d_0 (mm)	37	47	57
C	f (mm/r)	0.05	0.1	0.15
D	a_p (mm)	0. 5	1.0	1.5

Energy consumption of the variable-MRR machining process can be calculated as follows:

$$E_{MC} = \sum_{i=1}^{N} \left(\lambda \cdot \overline{v_{ci}}^{\alpha} \cdot \overline{f_i}^{\beta} \cdot \overline{a_{pi}}^{\gamma} \cdot \Delta t \right) \tag{10}$$

Where N is number of subintervals, Δt is the duration of each subinterval, s. $\Delta t = T/N$, T is duration of variable-MRR machining process, s.

When the three cutting parameters can be expressed as the function of time, then the material-cutting power of variable-MRR machining process can be written as formula (11).

$$P_{MC}(t) = \lambda \cdot v_c(t)^{\alpha} \cdot f(t)^{\beta} \cdot a_p(t)^{\gamma} \tag{11}$$

Where $v_c(t), f(t), a_p(t)$ are functions of cutting speed, feed rate, and depth of cut against time, respectively.

Based on formula (11), the energy consumption of the variable-MRR machining process can be derived by the energy method.

$$E_{MC} = \int_0^T P_{MC}(t)dt = \int_0^T \lambda \cdot v_c(t)^{\alpha} \cdot f(t)^{\beta} \cdot a_p(t)^{\gamma} dt \tag{12}$$

In the above model, the MRR is further broken down rather than be treated as a single variable. While fully considering the impact of each cutting parameter on the material-cutting power, the improved model will be more consistent with the material-cutting energy consumption behavior of actual machining.

3.2 Material-cutting energy model for typical variable-MRR process: end face turning

3.2.1 Material-cutting energy model of end face turning process

End face turning process is a typical variable-MRR process. In this section, the specific expressions of $\overline{\mathrm{MRR}}$, $v_c(t)$, $f(t)$ and $a_p(t)$ in the material-cutting energy model of variable-MRR process are established by taking end face turning process as an example. As shown in Fig. 5, the end face turning process can be divided into three stages: (1) cutter entering stage (① → ②), (2) fully cutting stage (② → ③) and (3) cutter exiting stage (③ → ④). The material-cutting energy consumption of the cutter exiting stage is very small due to its small cutting speed and short cutting time. Hence, the material-cutting energy of the cutter exiting stage is not considered in this study. Thus, the material-cutting energy model of the cutter entering stage and fully cutting stage are focused on in this section.

Stage 1: Cutter entering stage (① → ②)

For the cutter entering stage, the cutter is gradually cutting into the workpiece with the gradually decreasing cutting speed, increasing depth of cut, and constant feed rate. Functions of cutting speed and depth of cut against time are expressed by Eqs. (13) and (14), respectively.

$$v_c(t) = \frac{\pi n}{1000}\left(d_0 - \frac{2fn}{60}t\right) = v_0 - \frac{2f\pi n^2}{60000}t \tag{13}$$

Where d_0 is diameter of workpiece, mm; f is feed rate, mm/r; n is spindle speed, r/min; t is cutting time, s.

$$a_p(t) = a_p \cdot t / t_{en} \tag{14}$$

Where α_p is depth of cut, mm; t_{en} is duration of cutter entering stage, s.

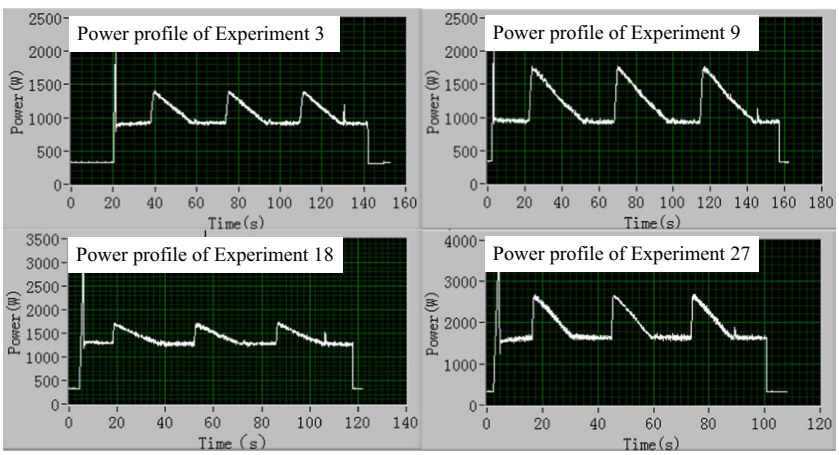

Fig. 6 Measured power profiles of four experiments

Table 3 Detailed material-cutting power data of experiment 3 at dry cutting environment

No	t (s)	v_c (m/min)	$P_{Total\text{-}cut}$ (W)				$P_{Air\text{-}cut}$(W)	P_{MC}(W)
			1st cut	2nd cut	3rd cut	Avg		
3-1	0.1	46.37	927.12	924.75	931.05	927.64	916.49	11.15
3-2	0.2	46.12	935.02	941.02	932.34	936.13	916.49	19.64
3-3	0.3	45.87	976.12	963.08	952.63	963.94	916.49	47.45
3-4	0.4	45.62	1009.96	986.15	993.86	996.66	916.49	80.17
3-5	0.5	45.37	1019.12	1024.54	1011.97	1018.54	916.49	102.05
3-6	0.6	45.12	1048.96	1041.85	1045.73	1045.52	916.49	129.03
3-7	0.7	44.87	1097.14	1056.17	1085.89	1079.73	916.49	163.24
3-8	0.8	44.62	1136.19	1093.82	1096.68	1108.90	916.49	192.41
3-9	0.9	44.36	1153.20	1132.91	1123.99	1136.70	916.49	220.21
3-10	1.0	44.11	1173.00	1156.75	1162.49	1164.08	916.49	247.59
3-11	1.1	43.86	1207.08	1202.89	1187.90	1199.29	916.49	282.80
3-12	1.2	43.61	1241.82	1233.44	1221.10	1232.12	916.49	315.63
3-13	1.3	43.36	1267.52	1251.85	1258.64	1259.33	916.49	342.84
3-14	1.4	43.11	1295.76	1293.37	1277.63	1288.92	916.49	372.43
3-15	1.5	42.86	1322.01	1314.23	1305.71	1313.98	916.49	397.49
3-16	1.6	42.60	1349.46	1338.30	1336.58	1341.45	916.49	424.96
3-17	1.7	42.35	1370.56	1365.01	1344.73	1360.10	916.49	443.61
3-18	1.8	42.10	1376.95	1367.38	1361.31	1368.55	916.49	452.06
…	…	…	…	…	…	…	…	…
3-183	18.3	0.63	964.57	963.82	966.12	964.84	916.49	48.35
3-184	18.4	0.38	951.68	950.45	946.85	949.66	916.49	33.17
3-185	18.5	0.13	953.33	937.25	950.78	947.12	916.49	30.63

$n = 400$ r/min; $d_0 = 37$ mm; $f = 0.15$ mm/r; $a_p = 1.5$ mm

The material-cutting power of cutter entering stage can be obtained by substituting the formula (13) and (14) into formula (11).

$$P_{MC} = \lambda \cdot \left(v_0 - \frac{2f\pi n^2}{60000} t \right)^{\alpha} \cdot f^{\beta} \cdot \left(a_p \cdot t / t_{en} \right)^{\gamma} \tag{15}$$

Stage 2: Fully cutting stage (② → ③)

For the fully cutting stage, the cutter is removing the material with constant feed rate, depth of cut, and decreasing cutting speed. The cutting speed is satisfied: $v_c(t) = \frac{\pi n}{1000}\left(d_0 - \frac{2fn}{60} t\right) = v_0 - \frac{2f\pi n^2}{60000} t$. Based on formula (11), the material-cutting power can be expressed as:

$$P_{MC} = \lambda \cdot \left(v_0 - \frac{2f\pi n^2}{60000} t \right)^{\alpha} \cdot f^{\beta} \cdot a_p^{\gamma} \tag{16}$$

According to Eqs. (15) and (16), the material-cutting power of end face turning process can be expressed with a piecewise function:

$$P_{MC} = \begin{cases} \lambda \cdot \left(v_0 - \frac{2f\pi n^2}{60000} t \right)^{\alpha} \cdot f^{\beta} \cdot \left(a_p \cdot t / t_{en} \right)^{\gamma} & , 0 \le t < t_{en} \\ \lambda \cdot \left(v_0 - \frac{2f\pi n^2}{60000} t \right)^{\alpha} \cdot f^{\beta} \cdot a_p^{\gamma} & , t_{en} \le t < t_{en} + t_{fcut} \end{cases} \tag{17}$$

Table 4 Curve fitting results (I-model)_dry

Coefficients	Value	Standard error	t-Value	Prob $>\|t\|$	Statistics
Λ	30.03755	0.28113	106.84735	0	R-square(COD)
A	1.03538	0.00213	487.05996	0	0.98492
B	0.79167	0.00227	348.86668	0	Adj. R-square
Γ	1.03915	0.0031	335.52449	0	0.98491

Table 5 ANOVA for material-cutting power (I-model)_dry

	DF	Sum of squares	Mean square	F value	Prob $>F$
Regression	4	5.48573E8	1.37143E8	272419.33771	0
Residual	8054	4.0546E6	503.42692		
Uncorrected total	8058	5.52628E8			
Corrected total	8057	2.68787E8			

Table 6 Fitting coefficients of material-cutting energy model for end face turning process

Item	Model	
Average-MRR based model	$E_{MC}=\lambda_0\cdot\overline{MRR}\cdot T,\ \left(\overline{MRR}=\frac{\pi d_0^2\times a_p}{4000\times T},\ T=t_{en}+t_{fcut}\right)$	
Cutting environment	Dry	Wet
Fitting coefficients	$\lambda_0=3060.256$	$\lambda_0=2964.198$
Improved energy model	$E_{MC}=\int_0^{t_{en}}\left[\lambda\cdot\left(v_0-\frac{2f\pi n^2}{60000}t\right)^{\alpha}\cdot f^{\beta}\cdot(a_p\cdot t/t_{en})^{\gamma}\right]dt+\int_{t_{en}}^{t_{en}+t_{fcut}}\left[\lambda\cdot\left(v_0-\frac{2f\pi n^2}{60000}t\right)^{\alpha}\cdot f^{\beta}\cdot a_p^{\gamma}\right]dt$	
Cutting environment	Dry	Wet
Fitting coefficients	$\lambda=30.038$, $\alpha=1.035$, $\beta=0.792$, $\gamma=1.039$	$\lambda=27.133$, $\alpha=1.078$, $\beta=0.845$, $\gamma=1.043$

Meanwhile, the following equations are satisfied:

$$v_0=\frac{\pi n}{1000}d_0,\quad t_{en}=\frac{l}{v_f}=\frac{a_p\cdot\cot\kappa_r}{nf/60},\quad t_{fcut}=\frac{d_0/2-l}{v_f}=\frac{d_0/2-a_p\cdot\cot\kappa_r}{nf/60} \tag{18}$$

Where v_0 is initial cutting speed, m/min; n is spindle speed, r/min; d_0 is diameter of workpiece, mm; t_{en} is duration of cutter entering stage, s; l is feed distance during cutter entering stage, mm; v_f is feed speed, mm/s; α_p is depth of cut, mm; κ_r is main angle; f is feed rate, mm/r; t_{fcut} is duration of fully cutting stage, s.

Material-cutting energy of the cutter entering stage can be calculated by formula (19).

$$E_{en}=\int_0^{t_{en}}\left[\lambda\cdot\left(v_0-\frac{2f\pi n^2}{60000}t\right)^{\alpha}\cdot f^{\beta}\cdot\left(a_p\cdot t/t_{en}\right)^{\gamma}\right]dt \tag{19}$$

Material-cutting energy of the fully cutting stage can be calculated by formula (20).

$$E_{fcut}=\int_{t_{en}}^{t_{en}+t_{fcut}}\left[\lambda\cdot\left(v_0-\frac{2f\pi n^2}{60000}t\right)^{\alpha}\cdot f^{\beta}\cdot a_p^{\gamma}\right]dt \tag{20}$$

Material-cutting energy of the end face turning process can be expressed as follows:

$$\begin{aligned}E_{MC}&=E_{en}+E_{fcut}\\&=\int_0^{t_{en}}\left[\lambda\cdot\left(v_0-\frac{2f\pi n^2}{60000}t\right)^{\alpha}\cdot f^{\beta}\cdot\left(a_p\cdot t/t_{en}\right)^{\gamma}\right]dt\\&\quad+\int_{t_{en}}^{t_{en}+t_{fcut}}\left[\lambda\cdot\left(v_0-\frac{2f\pi n^2}{60000}t\right)^{\alpha}\cdot f^{\beta}\cdot a_p^{\gamma}\right]dt\end{aligned} \tag{21}$$

For the end face turning process, the average-MRR can be expressed as follows:

$$\overline{\mathrm{MRR}}=\frac{\pi d_0^2\times a_p}{4000\times T} \tag{22}$$

Where T is duration of end face turning process, s; the equation $T=t_{en}+t_{fcut}$ is satisfied:

According to the formula (3) and formula (21), the material-cutting energy model for end face turning process are summarized in Table 1.

3.2.2 Fitting coefficients of material-cutting energy model

The coefficients of the average-MRR based model (abbreviated as A-model) and the improved energy model (abbreviated as I-model) are dependent on the co-effect of machine tool, cutter, and workpiece material, which are

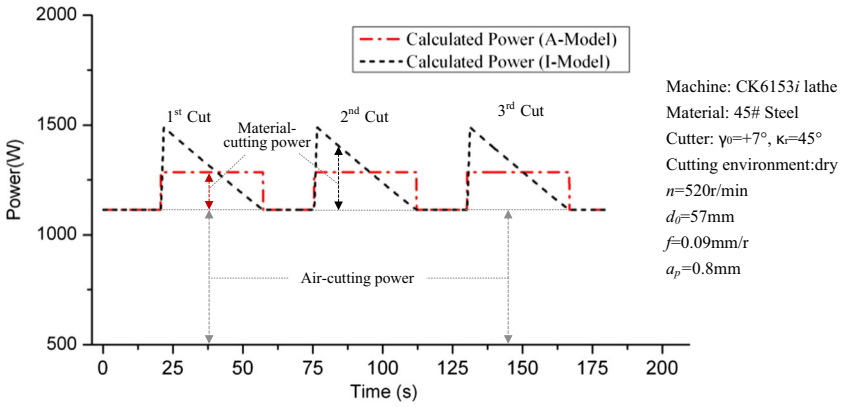

Fig. 7 Comparison of calculated power profiles of the A-model and I-model

Table 7 Parameter values of four test experiments

Parameters	Test 1	Test 2	Test 3	Test 4
Spindle speed (r/min)	520	620	500	620
Workpiece diameter (mm)	57	47	47	57
Feed rate (mm/r)	0.09	0.14	0.11	0.12
Depth of cut (mm)	0.8	0.6	0.5	0.7
Cutting environment	dry	dry	wet	wet
Cutter entering time (s)	1.03	0.41	0.55	0.56
Fully cutting time (s)	35.51	15.83	25.09	22.42
Total cutting time (s)	36.54	16.24	25.64	22.98

difficult to be obtained by theoretical analysis. Therefore, statistical analysis and curve fitting were conducted to obtain the coefficients of material-cutting energy model.

The material-cutting power is mainly influenced by cutting parameters (cutting speed v_c, feed rate f, and depth of cut a_p). Cutting speed changes during the end face turning process. The initial cutting speed is determined by spindle speed n and diameter of workpiece $d0$. Therefore, spindle speed n, diameter of workpiece d_0, feed rate f, and depth of cut a_p are selected as the process variables for design of experiment (DOE). Experiments were conducted on a CK6153*i* CNC lathe, which was manufactured by Jinan First Machine Tool Group Co., Ltd. of China. Blank material selected for the experiments was 45# steel (ASTM 1045 steel), which is widely used in structural parts (gears, shafts, etc.). The chemical composition of 45# steel is 0.44 % C, 0.23 % Si, 0.61 % Mn, 0.012 % P, 0.024 % S, 0.02 % Ni, 0.03 % Cr, 0.05 % Cu, 0.002 % Pb, and Fe (remainder). The chosen cutter was SNMG120408N-GU-AC725 ($\kappa_r = 45°$, $\gamma_0 = +7°$), which was manufactured by SUMITOMO of Japan. The levels of four experimental variables (n, d_0, f, a_p) are determined by comprehensively considering the performance of machine tool, characteristics of material, and recommended values given by cutter manufacturer, as shown in Table 2.

The experiments were arranged by using L27 (3^{13}) orthogonal array according to the Taguchi method. Taguchi method is an experimental strategy in which a modified and standardized form of DOE is used [44]. Each combination of cutting parameters was repeated three times to improve the reliability and accuracy of the observed data. The cutting environment refers to whether the cutting fluid is applied or not. In order to evaluate the impacts of the cutting fluid on the material-cutting energy, the experiments conducted in the condition of dry environment were repeated with cutting fluid. To record the power and energy data of CNC machine tool, an experimental setup was built by our research group. The experimental setup is composed of three voltage sensors (LEM LV25-P), three current sensors (LEM LA55-P), two NI-9215 data collecting cards, a CompactDAQ crate, and a LabVIEW

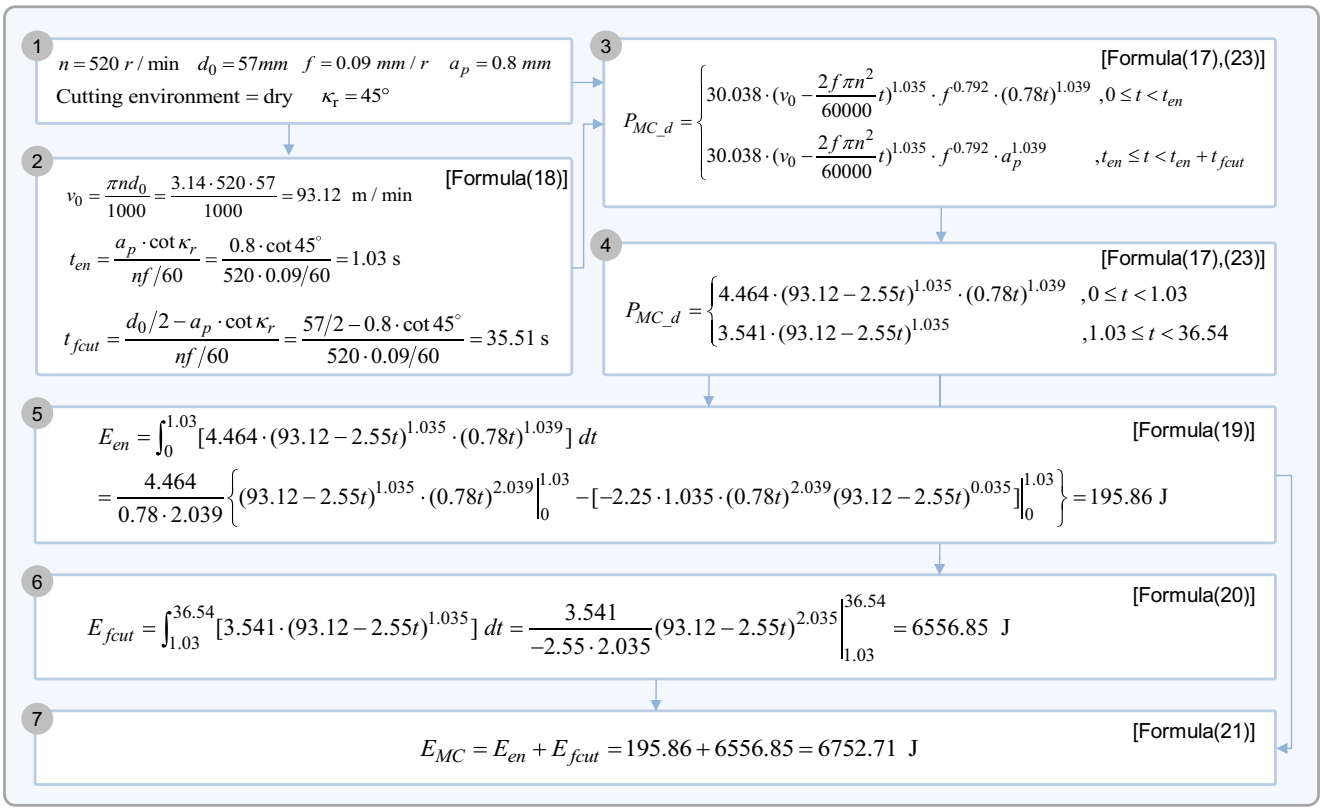

Fig. 8 Material-cutting energy calculation process for Test 1

Table 8 Calculation results of material-cutting energy for test groups (I-model)

No	Power model	E_{en} (J)	E_{fcut}(J)	$E_{Calculated}$ (J)	$E_{Measured}$ (J)	Accuracy
Test 1	$P_{MC\_d} = \{4.464\cdot(93.12-2.55t)^{1.035}\cdot(0.78t)^{1.039}, 0\le t < 1.03\ 3.541\cdot(93.12-2.55t)^{1.035}, 1.03\le t < 36.54$	195.86	6556.85	6752.71	6453.44	95.36 %
Test 2	$P_{MC\_d} = \{6.334\cdot(91.55-5.64t)^{1.035}\cdot(1.45t)^{1.039}, 0\le t < 0.41\ 3.725\cdot(91.55-5.64t)^{1.035}, 0.41\le t < 16.24$	82.55	3029.56	3112.11	2899.04	92.65 %
Test 3	$P_{MC\_w} = \{4.202\cdot(73.83-2.88t)^{1.078}\cdot(0.92t)^{1.043}, 0\le t < 0.55\ 2.039\cdot(73.83-2.88t)^{1.078}, 0.55\le t < 25.64$	56.05	2486.03	2542.07	2412.77	94.64 %
Test 4	$P_{MC\_w} = \{4.522\cdot(111.02-4.83t)^{1.078}\cdot(1.24t)^{1.043}, 0\le t < 0.56\ 3.117\cdot(111.02-4.83t)^{1.078}, 0.56\le t < 22.98$	166.37	5253.90	5420.27	5571.19	97.29 %

Accuracy = $(1-|E_{Calculated} - E_{Measured}|/E_{Measured}) \times 100$ %

interface. For detailed information about the experimental set-up, you can refer to reference [45]. The measured power and energy information were sorted in the SQL Server database 2005, and the measured power profiles of four experiments [3, 6, 18, 27] are shown in Fig. 6.

The sample rate of the experimental system was set to 10 Hz. The end face turning processes were executed on the CK6153i lathe while power and energy data were recorded by the abovementioned experimental setup. Since each set of experiment was repeated three times, the value of $P_{\text{Total-cut}}$ adopts the average value of three measurements. As shown in Table 3, taking experiment 3 as an example, the duration of cutter entering stage is 1.5 s and the duration of fully cutting stage is 17 s. Data observed during fully cutting stage (1.6~18.5 s) were selected to conduct data fitting. Experimental data of other 26 sets of experiments can also be processed with the similar method.

Curve fitting was carried out on Origin8.0® Software for all of the 27 groups of experimental data under a dry environment. Based on the formula (9), the curve fitting results and analysis of variance (ANOVA) were shown in Tables 4 and 5, respectively. According to Table 5, the coefficient $\lambda =$ 30.037559 and exponents $\alpha = 1.03538$, $\beta = 0.79167$, $\gamma =$ 1.03915. By substituting the above values (accurate to the third decimal place) into formula (17), the piecewise function of material-cutting power for the end face turning process at dry environment can be expressed as follows:

$$P_{MC\_d} = \begin{cases} 30.038\cdot\left(v_0-\dfrac{2f\pi n^2}{60000}t\right)^{1.035}\cdot f^{0.792}\cdot\left(a_p\cdot t/t_{en}\right)^{1.039}, & 0\le t < t_{en} \\ 30.038\cdot\left(v_0-\dfrac{2f\pi n^2}{60000}t\right)^{1.035}\cdot f^{0.792}\cdot a_p^{1.039}, & t_{en}\le t < t_{en}+t_{fcut} \end{cases} \tag{23}$$

The small P value (Prob = 0 < 0.05, 95 % confidence level) in ANOVA table indicates the strong correlation between P_{MC_d} and v_c, f, a_p. The R-square value is 0.98492, which indicates that the developed model could well describe the material-cutting power under various combinations of v_c, f, a_p.

The material-cutting energy of end face turning process at dry cutting environment can be expressed as follows:

$$E_{MC\_d} = \int_0^{t_{en}}\left[30.038\cdot\left(v_0-\frac{2f\pi n^2}{60000}t\right)^{1.035}\cdot f^{0.792}\cdot\left(a_p\cdot t/t_{en}\right)^{1.039}\right]dt + \int_{t_{en}}^{t_{en}+t_{fcut}}\left[30.038\cdot\left(v_0-\frac{2f\pi n^2}{60000}t\right)^{1.035}\cdot f^{0.792}\cdot a_p^{1.039}\right]dt \tag{24}$$

Similarly, fitting coefficients of improved energy model at wet cutting environment can be obtained. To compare the effectiveness of the improved energy model and average-MRR based model, fitting coefficients of the average-MRR based model were also obtained based on the same experimental data

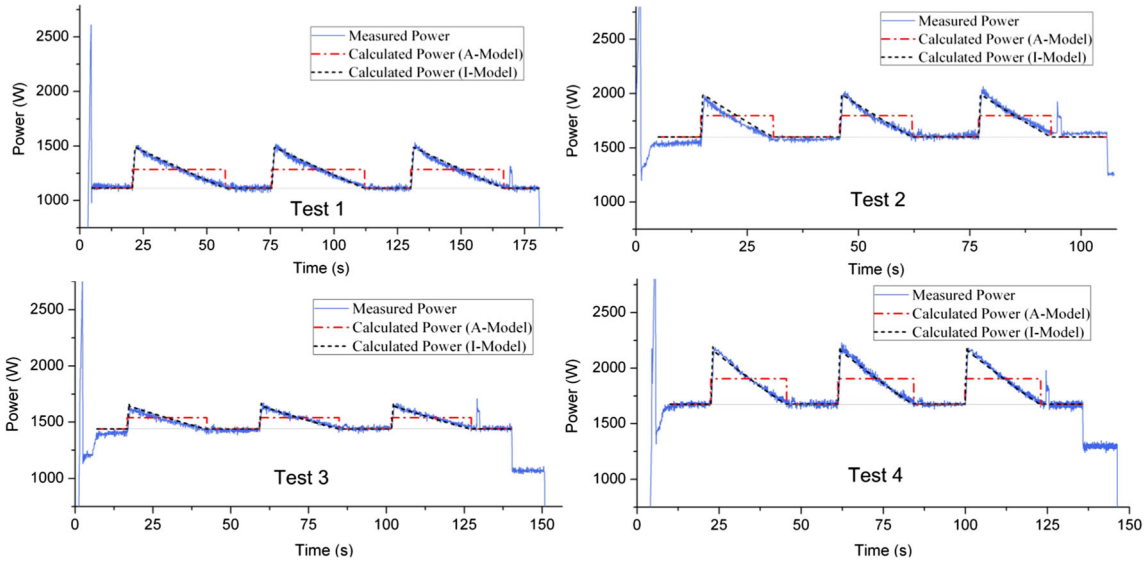

Fig. 9 Calculated power profiles with A-model and I-model vs. measured power profiles of the four tests

as the improved energy model. The obtained coefficients of material-cutting energy model for end face turning process are summarized in Table 6. Since the fitting coefficients vary between different machining processes (grooving, chamfering, milling process, etc.), the same modeling methodology needs to be repeated to other machining process [10].

When the fitting coefficients are determined, material-cutting energy of end face turning process under other combinations of cutting parameters can be calculated. Supposing the combinations of cutting parameters are ($n = 520$ r/min, $d_0 = 57$ mm, $f = 0.09$ mm/r, $a_p = 0.8$ mm), and the cutting process was repeated three times under dry condition. Based on the A-model, I-model, and the fitting coefficients in Table 6, the calculated power profiles can be obtained, as shown in Fig. 7.

4 Experimental study

To examine the validity of the improved energy model, four test experiments were conducted. As shown in Table 7, the parameter values of the four tests were chosen randomly and combinations of parameter value for these four tests were different with the data used for curve fitting. The material of the blank selected for the tests was 45# steel (ASTM 1045 steel). The four tests were conducted on the CK6153*i* CNC lathe, and each test was repeated three times to improve the reliability of the observed data. The selected cutter was SNMG120408N-GU-AC725 ($\kappa_r = 45°$, $\gamma_0 = +7°$).

According to the improved energy model in Section 3.1.2, the material-cutting energy calculation processes for test 1 are displayed in Fig. 8.

Following the same calculation processes, material-cutting energy for Test 2~Test 4 can also be obtained. The calculation results are listed in Table 8. The power and energy during four tests were recorded by the experimental setup built by our research group. The comparison of calculated power profiles with I-model and measured power profiles of the four tests are shown in Fig. 9. The calculation results of material-cutting energy with A-model are also obtained, which are shown in Table 9. The comparison of the calculated power profiles with

Table 9 Calculation results of material-cutting energy for test groups (A-model)

No	Power model	$\overline{MRR}$ (cm^3/s)	$\overline{P_{Mat-cut}}$ (W)	T(s)	$E_{Calculated}$ (J)	$E_{Measured}$ (J)	Accuracy
Test 1	$\overline{P_{MC\_d}} = 3060.256 \cdot \overline{MRR}$	0.056	170.98	36.54	6247.23	6453.44	96.80 %
Test 2	$\overline{P_{MC\_d}} = 3060.256 \cdot \overline{MRR}$	0.064	196.11	16.24	3185.63	2899.04	90.11 %
Test 3	$\overline{P_{MC\_w}} = 2964.198 \cdot \overline{MRR}$	0.034	100.30	25.64	2571.36	2412.77	93.43 %
Test 4	$\overline{P_{MC\_w}} = 2964.198 \cdot \overline{MRR}$	0.078	230.37	22.98	5294.74	5571.19	95.04 %

Accuracy = $(1-|E_{Calculated} - E_{Measured}|/E_{Measured}) \times 100$ %

A-model and I-model and measured power profiles of the four tests are shown in Fig. 9.

The impact of cutting parameters on material-cutting power is fully considered in the improved energy model (I-model), and the mathematical expression of this model is more complicated than the average-MRR based model (A-model). However, the basic input parameters of I-model are commonly used cutting parameters (cutting parameters v_c,f, a_p, spindle speed n), which are easily to be obtained. As the average-MRR is viewed as a single parameter in A-model, the dynamic characteristic of cutting power of cutting process is not reflected by A-model. The transparency of energy consumption of A-model is not satisfactory. However, the impact of cutting parameters on material-cutting power is considered by I-model, and the dynamic characteristic of cutting power of cutting process can also be reflected. The I-model improves the transparency of power and energy consumption of machining process and facilitates the exploration of high cutting power or low energy efficiency process. The I-model lays a solid foundation for energy optimization of machining processes. The accuracies of two models are both higher than 90.0 %, and the average accuracy of the I-model (95.0 %) is higher than that of the A-model (93.8 %). The calculation results of material-cutting energy with the above two models are shown in Fig. 10. Under the circumstances that the accuracy is not very important and just a rough result is required and the power details of cutting process are not concerned, the A-model can be employed to reduce the computational complexity. But when the high accuracy and the understanding of dynamic characteristic of cutting power for cutting process is required, the I-model is more appropriate.

Moreover, the maximum cutting power is more important than average cutting power of machining process when judging whether one machine meet the cutting requirements. Due to the fact that only the power provided by machine spindle is greater than the maximum cutting power of machining process, the machine is likely to meet the cutting requirements. If only the average cutting power is known while the maximum cutting power is unknown, one problem will exist: even the power provided by machine spindle is greater than the average cutting power, whether the power provided by machine spindle is greater than maximum cutting power or not is still not sure. Once the power provided by machine spindle is smaller than maximum cutting power, it will cause the machine spindle power shortage and make the spindle stop. Hence, the I-model can provide more accurate and effective power data compared to the A-model when judging whether one machine meet the cutting requirements.

5 Conclusions

The energy characteristic of variable-MRR machining process is more complicated than that of constant-MRR machining process due to the dynamically changing cutting parameters. In this paper, a modeling method for material-cutting energy of variable-MRR machining process is proposed. The variable-MRR machining process is decomposed into N subintervals by considering the dynamic changing cutting power. For each subinterval, the average material-cutting power is used to substitute the actual material-cutting power. Moreover, the total material-cutting energy is obtained by summing up the average material-cutting energy of each subinterval. Within each subinterval, the effect of each cutting parameter (v_c,f, a_p) on material-cutting power is fully considered rather than only taking into account the overall impact of MRR. The advantages of the improved energy model are as follows: (1) the variable-MRR machining process is divided into a large number of subintervals to analyze the power and energy consumption characteristic based on the thought of differential, which improves the transparency of material-cutting energy consumption of the variable-MRR machining process and makes it convenient to explore the high cutting power or low energy efficiency subintervals. (2) Within each subinterval, the function between material-cutting energy and three cutting parameters (v_c,f,a_p) is developed rather than taking the MRR as a single variable. This model is more constant with the actual situation and can well represent the energy consumption characteristic of variable-MRR machining process. (3) Variable-MRR machining process, as one of the

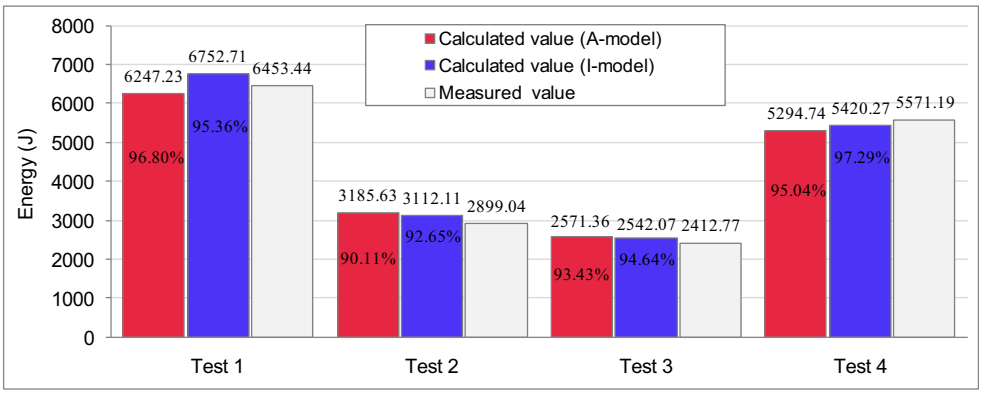

Fig. 10 Calculation results of material-cutting energy with A-model and I-model

common machining processes, the establishment of its material-cutting energy model can lay a solid foundation for energy modeling and energy optimization of machining processes. Experimental studies were carried out to obtain the fitting coefficients of the material-cutting energy model of variable-MRR machining process. The feasibility of the developed material-cutting energy model was verified by conducting material-cutting energy calculation of four test experiments.

Material-cutting energy model for variable-MRR machining process has been established in this study. The energy consumption of a typical machining process is mainly composed of energy consumption of non-cutting process and cutting process (constant-MRR cutting process and variable-MRR cutting process). Only the energy model of variable-MRR cutting process is combined with the energy models of non-cutting process and constant-MRR cutting process, and the complete energy model of machining process can be established. Further efforts will be conducted to establish an energy model of complete machining process based on the energy model of non-cutting process, constant-MRR, and variable-MRR cutting process. The energy optimization of machining process will be further researched based on such an energy model.

Acknowledgments The authors sincerely thank all the anonymous reviewers for their valuable suggestions on the improvement of our paper. Kaidong Yang from Tsinghua University, Saijun Shao from The University of Hong Kong, Qiang Wang from Engineering Training Center of Zhejiang University are particularly acknowledged for providing assistance during the experiments. Tao Peng from Zhejiang University is thanked for his efforts on revising this paper. This research is supported by the National Natural Science Foundation, China (No.51175464), National High Technology Research and Development Program of China (863 program, No. 2013BAF02B10) and Scientific Research Foundation of Shandong University of Science and Technology for Recruited Talents (No.2015RCJJ049).

References

1. Duflou JR, Sutherland JW, Dornfeld D, Herrmann C, Jeswiet J, Kara S, Hauschild M, Kellens K (2012) Towards energy and resource efficient manufacturing: a processes and systems approach. CIRP Ann - Manuf Technol 61(2):587–609
2. Calvanese ML, Albertelli P, Matta A, Taisch M (2013) Analysis of energy consumption in CNC machining centers and determination of optimal cutting conditions. In: Proceedings of 20th CIRP International Conference on Life Cycle Engineering, Singapore, pp 227–232.
3. Dahmus J, Gutowski T (2004) An environmental analysis of machining. 2004 ASME International Mechanical Engineering Congress and Exposition. ASME, Anaheim, CA, United states, pp 643–652
4. Mouzon G, Yildirim MB, Twomey J (2007) Operational methods for minimization of energy consumption of manufacturing equipment. Int J Prod Res 45(18–19):4247–4271
5. Rahimifard S, Seow Y, Childs T (2010) Minimising embodied product energy to support energy efficient manufacturing. CIRP Ann - Manuf Technol 59(1):25–28
6. International Energy Agency (IEA) (2007) Tracking industrial energy efficiency and CO_2 emission. OECD/IEA, Paris
7. Rajemi MF, Mativenga PT, Aramcharoen A (2010) Sustainable machining: selection of optimum turning conditions based on minimum energy considerations. J Clean Prod 18(10–11):1059–1065
8. Yan J, Li L (2013) Multi-objective optimization of milling parameters—the trade-offs between energy, production rate and cutting quality. J Clean Prod 52:462–471
9. Bhushan RK (2013) Optimization of cutting parameters for minimizing power consumption and maximizing tool life during machining of Al alloy SiC particle composites. J Clean Prod 39:242–254
10. Li L, Yan J, Xing Z (2013) Energy requirements evaluation of milling machines based on thermal equilibrium and empirical modelling. J Clean Prod 52:113–121
11. Behrendt T, Zein A, Min S (2012) Development of an energy consumption monitoring procedure for machine tools. CIRP Ann - Manuf Technol 61(1):43–46
12. Diaz N, Redelsheimer E, Dornfeld D (2011) Energy consumption characterization and reduction strategies for milling machine tool use. In: Proceedings of the18th CIRP International Conference on Life Cycle Engineering., pp 263–267
13. Jia S, Tang RZ, Lv JX (2013) Therblig-based modeling methodology for cutting power and its application in external turning. Comp Integ Manuf Syst 19(5):1015–1024
14. Li W, Kara S (2011) An empirical model for predicting energy consumption of manufacturing processes: a case of turning process. Proc Inst Mech Eng B-J Eng Manuf 225(9):1636–1646
15. Zhang Y (2013) Energy efficiency techniques in machining process: a review. Int J Adv Manuf Technol 71(5–8):1123–32
16. Fysikopoulos A, Pastras G, Alexopoulos T, Chryssolouris G (2014) On a generalized approach to manufacturing energy efficiency. Int J Adv Manuf Technol 73(9–12):1437–52
17. Peng T, Xu X (2014) Energy-efficient machining systems: a critical review. Int J Adv Manuf Technol 72(9–12):1389–406
18. Ma J, Ge X, Chang SI, Lei S (2014) Assessment of cutting energy consumption and energy efficiency in machining of 4140 steel. Int J Adv Manuf Technol 74(9–12):1701–8
19. Wang X, Luo W, Zhang H, Dan B, Li F (2015) Energy consumption model and its simulation for manufacturing and remanufacturing systems. Int J Adv Manuf Technol. doi: 10.1007/s00170-015-7057-7
20. Gutowski T, Murphy C, Allen D, Bauer D, Bras B, Piwonka T, Sheng P, Sutherland J, Thurston D, Wollf E (2005) Environmentally benign manufacturing: observations from Japan, Europe and the United States. J Clean Prod 13(1):1–17
21. Gutowski T, Dahmus J, Thiriez A (2006) Electrical energy requirements for manufacturing processes. In: Proceedings of the 13th CIRP International Conference on Life Cycle Engineering, Leuven, May 31st-June 2nd, pp 623–627.
22. Kara S, Li W (2011) Unit process energy consumption models for material removal processes. CIRP Ann - Manuf Technol 60(1):37–40
23. Balogun VA, Mativenga PT (2013) Modelling of direct energy requirements in mechanical machining processes. J Clean Prod 41:179–186
24. Lv JX, Jia S, Tang RZ (2014) Therblig-based energy supply modeling of CNC machine tools. J Clean Prod 65:168–177
25. Dietmair A, Verl A (2009) A generic energy consumption model for decision making and energy efficiency optimization in manufacturing. Int J Sustain Eng 2(2):123–133
26. Dietmair A, Verl A (2009) Energy consumption forecasting and optimization for tool machines. Modern Machinery Sci J 3:62–67

27. Mori M, Fujishima M, Inamasu Y, Oda Y (2011) A study on energy efficiency improvement for machine tools. CIRP Ann - Manuf Technol 60(1):145–148
28. Avram OI, Xirouchakis P (2011) Evaluating the use phase energy requirements of a machine tool system. J Clean Prod 19(6–7):699–711
29. Avram O, Stroud I, Xirouchakis P (2011) A multi-criteria decision method for sustainability assessment of the use phase of machine tool systems. Int J Adv Manuf Technol 53(5–8):811–828
30. Liu F, Liu J, He Y (2009) Automatic collection method of machining progress information for large-size workpieces based on reference power curve. J Mech Eng 45(10):111–117
31. Hu S, Liu F, He Y, Hu T (2012) An on-line approach for energy efficiency monitoring of machine tools. J Clean Prod 27:133–140
32. Tristo G, Bissacco G, Lebar A, Valentinčič J (2015) Real time power consumption monitoring for energy efficiency analysis in micro EDM milling. Int J Adv Manuf Technol 78(9–12): 1511–21
33. Li J, Lu Y, Zhao H, Li P, Yao Y (2013) Optimization of cutting parameters for energy saving. Int J Adv Manuf Technol 70(1–4): 117–124
34. Wang Q, Liu F, Wang X (2013) Multi-objective optimization of machining parameters considering energy consumption. Int J Adv Manuf Technol 71(5–8):1133–1142
35. Campatelli G, Lorenzini L, Scippa A (2014) Optimization of process parameters using a response surface method for minimizing power consumption in the milling of carbon steel. J Clean Prod 66: 309–316
36. Jia S, Tang RZ, Lv JX (2014) Therblig-based energy demand modeling methodology of machining process to support intelligent manufacturing. J Intell Manuf 25(5):913–931
37. Diaz N, Ninomiya K, Noble J, Dornfeld D (2012) Environmental impact characterization of milling and implications for potential energy savings in industry. Procedia CIRP 1:518–523
38. Bayoumi AE, Yücesan G, Hutton DV (1994) On the closed form mechanistic modeling of milling: specific cutting energy, torque and power. J Mater Eng Perform 3(1):151–158
39. Liu F, Xu ZJ, Dan B (1995) Energy characteristic of mechanical machining system and its application. China Machine Press, Beijing
40. Kordonowy DN (2002) A power assessment of machining tools, bachelor of science thesis in mechanical engineering. Massachusetts Institute of Technology, Cambridge, Massachusetts
41. Stute H, Limed EVD (1995) Transmissions and efficiencies for machine tools. Industrial indicator. 5–8
42. China Machinery Industry Federation (1997) Machining technology handbook. China Machine Press, Beijing
43. Ai X, Xiao SG (1994) Handbook of cutting parameters, 3rd edn. China Machine Press, Beijing
44. Camposeco-Negrete C (2013) Optimization of cutting parameters for minimizing energy consumption in turning of AISI 6061 T6 using Taguchi methodology and ANOVA. J Clean Prod 53:195–203
45. Jia S, Tang RZ, Lv JX (2014) Machining activity extraction and energy attributes inheritance method to support intelligent energy estimation of machining process. J Intell Manuf. doi: 10.1007/s10845-014-0894-7